

An Empirical Expression for Line Widths of Ammonia from Far-Infrared Measurements

J. R. Brown and D. B. Peterson

mail stop 183-301, Jet Propulsion Laboratory

California Institute of Technology

Pasadena, CA 91109

Manuscript pages 17

Tables 7

Figures 5

Submitted to J. M. S.

Running head:
Expression for Ammonia Line Widths

Send Galley Proofs to:

Dr. Linda R. Brown

mail stop 183-301

Jet Propulsion Laboratory
4800 Oak Grove Drive
California Institute of Technology
Pasadena, CA 91109

You may contact me by

Telephone 818-354-2940

Fax 818-354-5148

Email linda@atmosmips.jpl.nasa.gov

Abstract

The hydrogen- and self-broadened line widths of $^{116}\text{NH}_3$ ground state transitions with $J, K = 1, 0$ to $10, 10$ have been measured at 0.006 cm^{-1} resolution using a Bruker spectrometer between 40 to 210 cm^{-1} . These experimental widths have been reproduced to 2,4% and 11% respectively using an heuristically derived expression of the form

$$Y = a_0 + a_1 J'' + a_2 K'' + a_3 J''^2 + a_4 J'' K''$$

where J'' and K'' are the lower state symmetric top quantum numbers. This function has also been applied to the measured widths of the 58 transitions of v_{v} , each broadened by N_2 , O_2 , Ar , H_2 , and He (Pine et al., *J. Quant. Spectrosc. Radiat. Transfer* 50, 337-348 (1993)) and NI_3 (Markov et al., *J. Quant. Spectrosc. Radiat. Transfer* 50, 167-178 (1993)). The rms of the observed minus calculated widths are $\pm 5\%$ or better for the five foreign broadeners. For the self-broadening case, the expression fails to reproduce the $K = 0$ data. The values of the fitted constants suggest that for some broadeners the expression might also be written as

$$y = a_0 + b_1 J'' + b_2 (J'' - K'') + b_3 J''(J'' - K'')$$

introduction

Accurate knowledge of the foreign gas broadening of ammonia is required for planetary remote sensing (1). For example, N₂ and O₂ are the relevant species for the terrestrial troposphere while 1 I₂- and 1 He- broadening dominate the atmospheres of the outer planets. Unfortunately, such information is rather limited. Most researchers have reported experimental broadening coefficients for a relatively small number of transitions (see (2-4) for a review), and many width measurements have accuracies of only 10 to 30% (5,6). “There are two notable exceptions at high resolution which have” provided measurements to $\pm 4\%$. Margolis and Poynter (7) have measured hydrogen broadening for 203 transitions at 200 K in the ν_2 band at 11 μm region. Most recently, Pine et al, (8) and Markov et al. (9) have obtained experimental widths for 58 selected lines of ν_1 near 3 μm ; each transition was broadened by 1 I₂, N₂, O₂, 1 Ic, Ar and NH₃ (self-broadening). In these high resolution studies, the widths varied significantly as a function of the rotational quantum numbers J and K in the range of J equal 0 to 12.

Unfortunately, the results of these studies are not easily applied to atmospheric monitoring because the theoretical models such as the Anderson-Tsao-Curnutte theory (10,11) are unable to reproduce such accurate data. For example, in the theoretical modeling of self-broadening shown by Markov et al. (9), the differences between observed and calculated widths ranged from 5 to 25% ($\%(\text{o}-\text{c})/\text{c}$). Without a good theory, widths of the many unmeasured transitions can not be accurately calculated.

The present study was made to support planetary applications. Its goal was to obtain

a complete and accurate set of empirical 1 IZ-broadened widths at room temperature for the parallel band transitions in the rotational R branch between 35 and 220 cm⁻¹. in the present data, the widths were found to vary as a function of J and K in a manner seen in the previous high resolution studies. During the analysis of these data, it was noticed that a simple five-term expression involving J[“] and K[“] reproduced the observed foreign broadening measurements from this and earlier studies.

Experimental Details

Spectra were recorded in the 35 to 240 cm⁻¹ region with the 1 IR 120 Bruker Fourier transform Spectrometer (FTS) at the Jet Propulsion Laboratory. For these, a helium-cooled bolometer detected the infrared signal from a Hg-Arc source passing through a mylar beamsplitter. Each spectrum was integrated from 12 to 15 hours, but it was recorded in subsets of 3 to 4 hours duration so that the ammonia abundance could be monitored. The final spectra with an unapodized resolution of 0.0056 cm⁻¹ had signal-to-noise ratios 800:1 or better. In most cases, an empty cell scan was recorded for ratioing, although the FTS chamber was evacuated with a cryopump to remove residual H₂O. Figure 1 shows a typical example of a resulting transmission spectrum. in this region, the spectrum is dominated by R branch manifolds occurring every 19 cm⁻¹. Each manifold contains two sets of inversion transitions (a-s and s-a at each J and K) separated by 1 cm⁻¹; the R₅ lines are 119 cm⁻¹ apart shown in Fig. 2.

One of two glass absorption cells with wedged, high-density polyethylene windows was

used inside the sample compartment of the I^{FT}S. Sample pressures were monitored using Baratron capacitance pressure gauges accurate to 20.596 or better. The sample temperature was taken to be the same as the I^{FT}S temperature. The ammonia sample was isotopically enriched (99.95%) ¹⁴N₁, and the hydrogen sample was ultra-pure grade. The gas conditions are summarized in **Table I**, and a portion of four spectra is shown in **Fig. 2**. Initially one spectrum of 1 ICl and two of pure NH₁ were recorded with a 1.06 ± 0.05 cm length cell to validate the I^{FT}S performance and the data reduction software. These spectra were then used to calibrate the line positions, to check the quality of the 1 HITRAN (12) prediction and to obtain ammonia self-broadened widths. The catalog was found to be reliable for positions within ± 0.0002 cm⁻¹ and a few percent for intensities of the 0000-0000 transitions. The partial pressures of NH₃ listed in '1'able I were obtained by matching the observed R_s manifolds to the corresponding synthetic spectra computed with the 1992 HITRAN linelist. During comparisons done between 80 and 200 cm⁻¹, it was noticed that the 0100-0100 (i.e., v₂-v₂) intensities are calculated too high by nearly a factor of two.

Data reduction was done using a non-linear least squares curve-fitting of the spectral data.(13) For this, a synthetic spectrum was computed using line positions and intensities from the 19921 HITRAN database and a constant default Lorentz width in the Voigt profile. The 1 ICl lines were used to check that the line shapes were symmetric and to determine the instrument function, as was done by Pickett et al. (14). The spectra] and the continua parameters were then iterated to reduce the differences between the observed and synthetic spectra. Correct modelling of under-resolved HCl lines required the application of the finite aperture correction; with it, the ratios of the measured 113s~l/1137Cl intensities were

generally 3.12 ($\pm 3\%$). Although insignificant, this same correction was applied for the retrieval of ammonia positions, intensities and widths. The parameters from the two pure sample scans are compared in Table II; the upper panel shows that the intensities and widths of unblended features obtained from two different optical densities agree within 1%.

In the lower panel, the corresponding values for these inversion pairs are shown, indicating that experimental precision is 1% for isolated lines and 5% or better for blended lines (generally the K = O and 1) in this region.

Following these checks, six spectra of hydrogen-broadened ammonia were recorded using a 26.3 cm glass cell with total pressures of 50 to 388 torr; a sample from four optical densities is shown in Fig. 2. Lower H₂ pressures were selected to avoid giving rise to line mixing (1 S) so that good line widths could be obtained with Voigt profiles. Mixtures of the NH₃ and H₂ were made in a glass manifold and then feed into the absorption cell without purification. To allow equilibrium to occur, the sample was placed in the cell for one to four hours before any scans were taken. During the scanning, the ammonia abundance remained fairly constant, but the partial pressure of water within the absorption cell was found to increase. To compensate for the residual absorption indicated by solid circles in Fig. 2, additional parameters were added in the curve-fitting retrievals (e. g. the feature at 120.08 cm⁻¹ in Fig. 3). The self-broadening widths were held fixed to values obtained from the two pure gas spectra. To initialize the retrievals, a constant H₂-width of 0.08 was always assumed. In all cases, the adjustment of line parameters was done in steps. First, the widths and positions of up to 16 transitions were alternately iterated with the intensities held fixed until near convergence was achieved (usually in 3 or 4 iterations).

Then on the final iteration, all three quantities were adjusted. An example of the resulting spectral fit is shown in Fig. 3 where the observed and calculated spectra are overlaid with the residuals plotted above.

Results

The measured broadening coefficients for 116 ground state rotational R branch transitions in the far-infrared are presented in Table 1. The first column gives the rotational assignment: inversion state (a or s), AJ, J“, K“. The second through fourth columns list the observed positions, the relative intensities and their corresponding, experimental error (%err) followed by the ratio of the calculated to the observed intensity. The column labelled *n_{num}* gives the number of spectra from Table 1 used for the average. The remaining columns show the observed widths, their experimental errors in percent and the observed - calculated differences in percent for the H_2 - and self-broadening, respectively. The observed widths are in $\text{cm}^{-1}/\text{atm}$ and the % experimental error is the rms of the individual measurements. As seen in Table I, the temperatures of the gas samples vary from 293.6 K to 298, K. The temperatures of the H_2 - and self-broadened widths are assumed to be 296 K and 294 K, respectively, with an uncertainty of ± 3 . K. Since the true temperature dependence of the widths is not known, the individual measurements are not normalized to a common temperature before averaging; this introduces an additional uncertainty of 10%.

The accuracies of the measurements vary. The best measurements meet four

criteria: 1) the experimental error (rms) is less than 3% 2) at least 4 of the 6 spectra are used 3) the ratio of the calculated to retrieved intensity is close to 1.00 ($\pm 3\%$) and 4) the ratios of the widths and intensities of the inversion pairs are close to 1.00, as in Table 11. Blending is generally the reason for the poorer quality measurements. In a few cases, measurements are taken from only two spectra because the line overlap is so severe that only the lowest pressure runs can be used. Measurements of R_1 and R_2 from the 35 to 60 cm^{-1} region are particularly suspect because the transitions falls on the far wings of the band pass where the signal to noise is 40:1. Future investigations may eventually reveal that the experimental uncertainties of the R_1 and R_2 widths are much larger than our statistics suggest. They are included to provide a set of R branch widths involving nearly all the quantum numbers from $J = 1$ to 10. The quantum number variation from $K'' = J''$ to $K'' = 0$ is between 40 and 60%, as in Refs. 6-8. The maximum width occurs at $J'' = K''$ and the minimum at $K'' = 0$. At high J'' , the widths of $K'' = 0$ and $K'' = 1$ are nearly equal within experimental error.

One remarkable result of the Pinc et al. study (7) is their Fig. 3 showing that the widths of five foreign broadeners (N_2 , O_2 , Ar, H_2 , and He) nearly lie along straight lines when plotted as a function of $J'' + 0.2 (J'' - K'')$. A similar presentation is given in Fig. 4 to emphasize the variation of the far-infrared H_2 -widths with rotational quantum numbers. in this plot, widths of the same J (with $K = 0$ to $J = K$) lie along individual lines with different slopes. The fact that all but two ($J = 1, 2$) of these lines have nearly the same intercept suggests that a function exists to model the data. The expression $\gamma = a_0 + a_1 J'' - a_2 K''$ fails to fit the transitions involving K'' near 0 and K'' near J'' ; to compensate

for a parabolic pattern in the residuals, we introduce two extra terms, $J''2$ and $J''K''$ to obtain Eq. 1.

$$y = a_0 + a_1 J'' + a_2 K'' + a_3 J''^2 + a_4 J''K'' \quad (1)$$

Using Eq. 1, the 112- and self- broadened widths of the far-infrared ground state transitions are fitted to rms values of 2.4.% and 11.0%, respectively. Table 111 lists the individual residuals in percent, and Figure 5 plots the % (observed - calculated)/calculated widths as a function of J'' . Equation (1) is also applied to all the room temperature data at $3\mu\text{m}$ (7,8). Table IV gives observed widths in $\text{cm}^{-1}/\text{MPa}$ ($= 9.869 \text{ cm}^{-1}/\text{atm}$) at 296 K and the percent observed minus calculated differences $\%(\text{o}-\text{c})/\text{c}$ for the 58 transitions with six broadeners: N_2 , O_2 , Ar, He , HHe and NH_3 . The rms values range from 3.2% for N_2 to 8.0% for NH_3 (self). For both studies, Equation (1) fails to reproduce the self-broadening widths at low K and low J , in the present study, these transitions are blended and thus more difficult to measure. In the Pine et al. study, there is limited data. However, the residuals differences between the observed and calculated self-broadened widths are too great to be the result of experimental error. The 203 P,Q and R branch H_2 -broadened widths of Margolis and Poynter (6) are fitted to Eq. 1 with less success. The significant differences between the P, Q and R widths can not be removed by adjusting the five constants. Therefore, each branch is fitted separately; the corresponding parameters for the widths at 200 K are listed at the bottom of Table V.

The fitted constants for Eq. 1 and their corresponding uncertainties are listed in

Table V along with the %rms and number of data points included. Most of the parameters are statistically well-determined. The fitted constants themselves have interesting regularities. Except for a_3 of Ar, all the signs of the corresponding terms are the same with a_1 and a_4 being negative. in addition, a_3 is nearly equal but opposite of a_4 . These observations suggest that the relation might be also expressed as

$$\gamma = a_o + b_1 J'' - a_2 (J'' - K'') - t a_3 J'' (J'' - K'') \quad (2)$$

where $b_1 = a_1 + a_2$

Discussion

No attempt is made to connect the fitted constants to theoretical models, but it is remarkable that this simple expression fits the available data of so many broadeners. The success should be attributed to the fact that the data is limited by the range in ΔJ and J, K . The present work involves only R branch transitions, and the Pine et al. study reports mostly Q branch lines. The rotational quantum numbers span only up to $J, K = 10, 10$; the behavior of the widths at higher J can be quite different, as seen in recent studies of a heavier species like CH_3Cl (16). in addition, with the Pine et al. results, the parallel band transition probabilities make it difficult to measure the low-K Q-branch transitions so that at higher J less than half of the possible K values are available for VI.

In some species, the broadening coefficients vary not as a function of lower state J'' , but of $|m|$ where $m = -J''$) J'' and $J'' + 1$ for P, Q and R branch lines respectively. That is, the widths of P_4 , Q_4 and R_3 are predicted (16; for CH_3Cl) or observed (17; for NO) to be the same. However, this dependence on $|m|$ is not true for ammonia. For example, in the $3 \mu\text{m}$ data (8,9), there are a few R branch lines that can be compared directly to Q branch widths of the same m and K. Table VI lists the measurements for three cases. The left columns show the assignment with the value of m included. The columns that follow give the measured widths in $\text{cm}^{-1}/\text{MPa}$. The values for inversion pairs (a and s) are shown whenever possible to provide an assessment of measurement precision. Below each m set are written the differences between the R and Q branch widths ($\% (R-Q)/Q$). While a few entries agree within the experimental uncertainty of 1 to 3%, the differences are generally much larger, particularly for self-broadening. In the v_2 band, this lack of dependence of the widths on $|m|$ is also seen by Margolis and Poynter (7) for H_2 -broadening at 200 K. Unfortunately, the v_2 results are the only ammonia dataset that provides numerous and accurate P, Q, and R branch widths through a large range of J and K. If more measurements were available for all branches with different broadeners, then a more general empirical expression might be derived.

Since the present, the Pine et al. (8), and the Margolis and Poynter (6) studies all report measurements of I_2 -broadening in three different parallel bands (rotational, VI and v_2), the vibrational dependence of the widths can be examined. The averaged ratio of Pine et al. to the present H_2 -widths for the 10 R branch transitions of v_1 through $J'' = 3$ is 1.04 (2), indicating small vibrational dependence. Direct comparison with H_2 -

broadened widths of v_2 is more complicated since the measurements are reported at 200 K, and it is difficult to separate the vibrational from the temperature dependence. **Table VII** shows the present and v_2 widths and their ratios for the R_4 and R_6 manifolds. The ratios in column 4 are not constant (like the v_i /present ratios) but decrease with decreasing K'' . This could mean that the rotational variation of the widths is different for different vibrations, as discussed by Pine et al., but there is another possibility. This variation might also arise from a rotational dependency of the temperature coefficient "n" in

$$\gamma_{\text{temp } 1} = \gamma_{\text{temp } 2} (\text{temp } 2/\text{temp } 1)^n \quad (3)$$

The "n" coefficient is difficult to measure because small errors in the widths and the temperatures greatly affect the exponent obtained; for example a combined variation of 5% in the above ratios causes a 15% uncertainty for n. Pine et al. used the ratio of corresponding Q branch transitions of v_1 and v_2 to obtain an averaged n of 0.69. The ratio of common R branch lines of the present and v_2 lines give n = 0.73 (if a handful of points are excluded). As seen in **Table VI 1**, the computed n values decreases with decreasing K'' . However, this variation is not seen in five seemingly-accurate measurements of v_2 P branch widths (4). Other H_2-NH_3 data does not resolve whether this variation is from J,K dependence of n or not because they involve limited measurements of perpendicular transitions (Broquier et al, (18)) or because the experimental accuracies are too poor (Baldacchini et al. (S,6)). More investigation is needed to address this question.

In the 1992 HITRAN molecular database (12), the ammonia air- broadening

coefficients are set to a constant value, regardless of quantum number. In the interim, until a successful application of theoretical models can be made, Equation (1) and the self-, N₂- and O₂- fitted constants in Table V obtained from fitting the 3 μm (8,9) data have been used to predict values for the self- and air-broadening for the revised ammonia line parameters. Several caveats apply. First, the fitted data contain mostly Q branch widths; Given the AJ variation, the computed widths will likely be too low in the R branch and too high in the P branch, Since low K values at higher J are not observed by Pine et al., the computation should deviate much more for these cases,

Conclusion

Prediction of broadening coefficients to only $\pm 15\%$ is not adequate for accurate tropospheric remote sensing (1). We hope that as a result of this paper, an earnest effort will be undertaken to model the collective ammonia broadening data and perhaps define better expressions to calculate line widths. Ammonia is a good candidate for such studies because the inversion gives rise to pairs of transitions that can provide an experimental basis for judging measurement precision. For the present, the good accuracies of these existing measurements and the potential for calculating widths to within experimental accuracies have been demonstrated. However, the AJ dependence of the widths is more complicated than current application of theory or these simple expressions indicate. To achieve better understanding, there should be more width measurements with different broadeners, and these should be accurate (f: 3%) and complete P, Q and R branches for all J and K).

For 1I_2 - broadening of NH_3 , the vibrational dependence of widths for three parallel bands is small at low J . No judgement is being made about the behavior of perpendicular and hot bands widths. There is an indication that the temperature dependence of the widths might vary with J and K , and this possibility should be investigated in future studies. Accurate and complete 1Iz -broadened widths at room temperature are now available for the far-infrared R-branch. It is observed that the predicted intensities of the v_2-v_2 difference band are too high on the molecular database by nearly a factor of two.

Acknowledgements

The research reported in this paper was performed at the Jet Propulsion Laboratory, California Institute of Technology, under contract with the National Aeronautics and Space Administration. We thank A. Pine for providing electronic versions of the v_1 data.

References

1. M. A. 11, Smith, and 1.. 1.. Gordley, *J. Quant. Spectrosc. Radiat. Transfer* 29, 413-418 (1983),
2. P. Varanasi, *J. Quant. Spectrosc. Radiat. Transfer* 39, 13-2S (1988).
3. M. A. 11. Smith, C. P. Rinsland, V. Malathy Devi, 1.. S, Rothman, and K. Narahari Rae, *Intensities and Collision-broadening parameters from infrared spectra: an update*, in Spectroscopy of the Earth's Atmosphere and Interstellar Medium, K. N. Rao and A. Weber Eds., Ch. 3, pp 97-151, Academic Press, Boston, Ma, (1992).
4. P. Varanasi and A, Gopalan, *J. Quant. Spectrosc. Radiat. Transfer* 49, 383-388 (1993).
5. G. Baldacchini, A. Bizzarri, I.. Nencini, V. Serge, G. Buffa, and O. Tarrini, *J. Quant. Spectrosc. Radiat. Transfer* 43, 371-380 (1990),
6. G. Baldacchini, G. Buffa and Tarrini, *Il Nuovo Cimento* 13, 719-733 (1991).
7. J. S. Margolis and R. L. Poynter, *Appl. Opt.* 30, 3023-3028 (1991)
8. A. S. Pine, V. N. Markov, G. Buffa, and O. Tarrini, *J. Quant. Spectrosc. Radiat. Transfer* 50, 337-348 (1993).
9. V, N. Markov, A. S. Pine, G. Buffa, and O. Tarrini, *J. Quant. Spectrosc. Radiat. Transfer* so, 167-178 (1993) .
- 10.P. W. Anderson, *Phys. Rev.* 76647-661 (1949).
- 11, C. J. Tsao and B. Curnutte, *J. Quant. Spectrosc. Radiat. Transfer* 2, 41-91 (1 962).
12. 1.. S. Rothman, R. R. Gamache, R. 11, Tipping, C. P. Rinsland, M. A, 11. Smith, D. C. Benner, V. M. Devi, J.-M, Flaud, C. Camy - Peyret, A. Perrin, A, Goldman, S. “1’.

- Massie, L.. R., Brown, and R. A. Toth, *J. Quant. Spectrosc. Radiat. Transfer* 48, 469-507 (1992).
13. L. R. Brown, J. S. Margolis, R. I I. Norton, and B. Stedry, *Appl. Spectrosc.* 37, 287-292 (1983).
14. H. M. Pickett, D. B. Peterson, and J. S. Margolis, *J. Gee. Res.* 97,20787-20793 (1992).
15. A. Levy, N. Lacome, and C. Chackerian, Jr., *Collisional Line Mixing, in Spectroscopy of the Earth's Atmosphere and Interstellar Medium*, K. N, Rao and A. Weber Eds., Ch. 3,pp 97-151, Academic Press, Boston, Ma, (1992).
16. J. -P. Bouanich, G. Blanquet, and J. Walrand, *J. Mol. Spectrosc.* 161, 416-426 (1993).
17. M. N, Spencer, C. Chackerian, Jr., L. P. Giver, and L., R, Brown, *J.Mol.Spectrosc.* 168, 506-524 (1994).
18. M. Broquier, A. Picard-Bersellini, H. Aroui, and G. I). Billig, *J.Chem. Phys.* 88, 1551-1556 (1988).

FIGURES CAPTIONS

1. The spectrum of pure ^{14}NI 1₃ between 70 and 230 cm⁻¹ at 0.0056 cm⁻¹ resolution. The sample pressure is 4 torr at 294 K, and the optical path is 1.06 cm. The interval contains parallel band rotational transitions (0000-0000) from R₃ to R₁₀. The weaker features belong to the (0100-0100) hot band of ammonia and residual water.
2. Four spectra of H₂-broadened 13 in the region of the R₅ manifolds. In the upper trace, lower state K'' is labelled above each transition, and residual water lines are indicated by solid circles.
3. The curve-fitting of the 50 torr H₂-broadened ^{14}NI 1₃ scan. The observed and synthetic spectra are overlaid in the bottom panel with the residual differences in percent plotted above.
4. The observed H₂-broadened widths of ^{14}NI 1₃ in cm⁻¹/atm at 296 K from the present study vs J'' + 0.2 (J''-K''). The widths of the same J'' lie along separate lines having nearly the same Y-intercept. This pattern suggests the existence of an empirical expression to reproduce these measurements.
5. The computed residuals in percent (observed-calculated) /calculated for the present H₂-broadened widths of ^{14}NI 1₃. The rms for 116 transitions is 2.4%.

TABLES

- I. Experimental Conditions of the Ammonia Spectra
- II. Retrieved Parameters for R_s from Two Pure NH₃ Spectra
- III. The Far-Infrared H₂- and Self-broadened Widths of ¹⁴N113
- IV. Fitted R and Q Branch widths of V_j
- V. Fitted Constants for Equation (1) in units of cm⁻¹/atm
- VI. R and Q Branch Widths of v₁ with the Same | m |
- VII. Vibrational or Temperature Dependence?

SYMBOLS

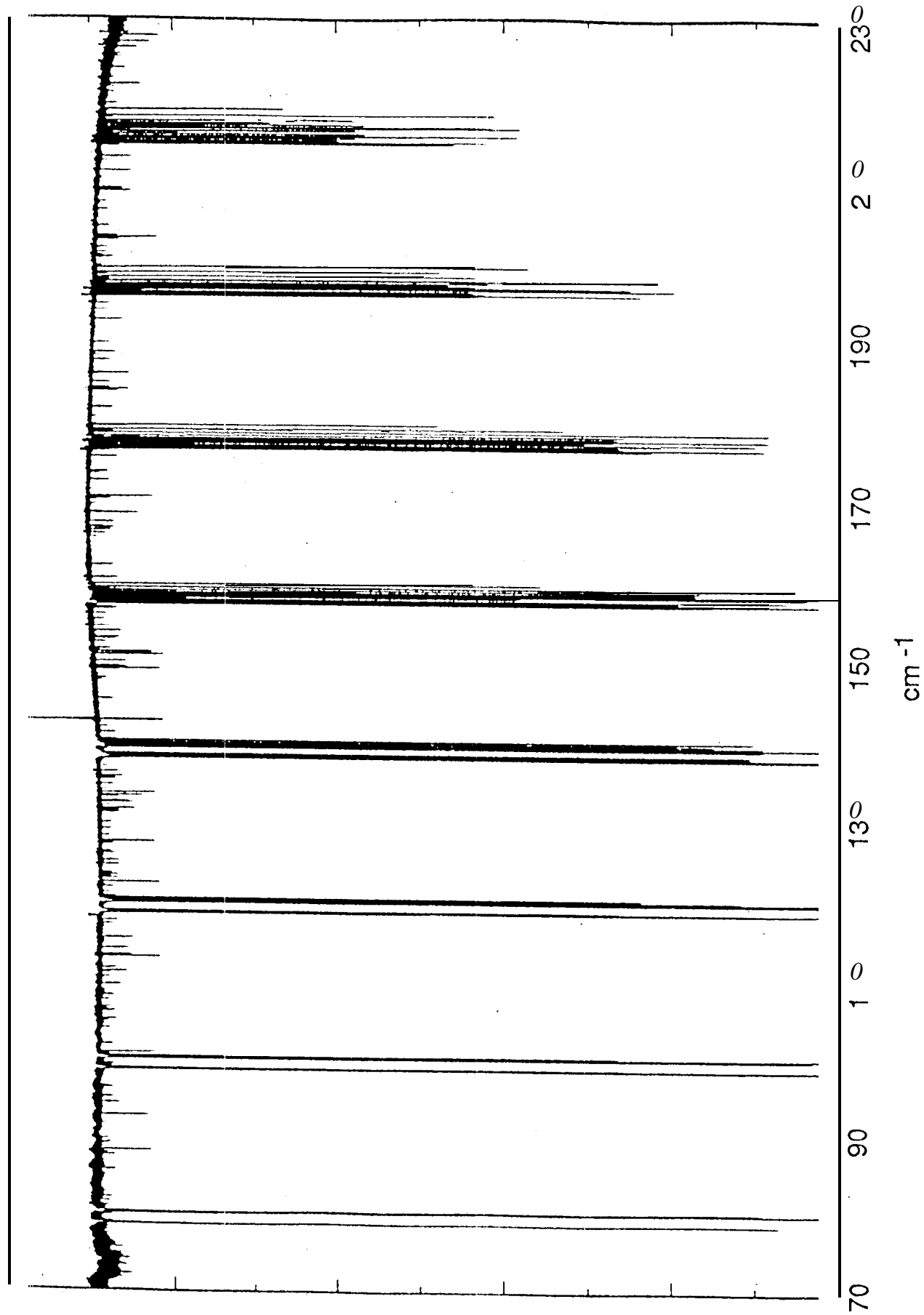
v nu

μ mu

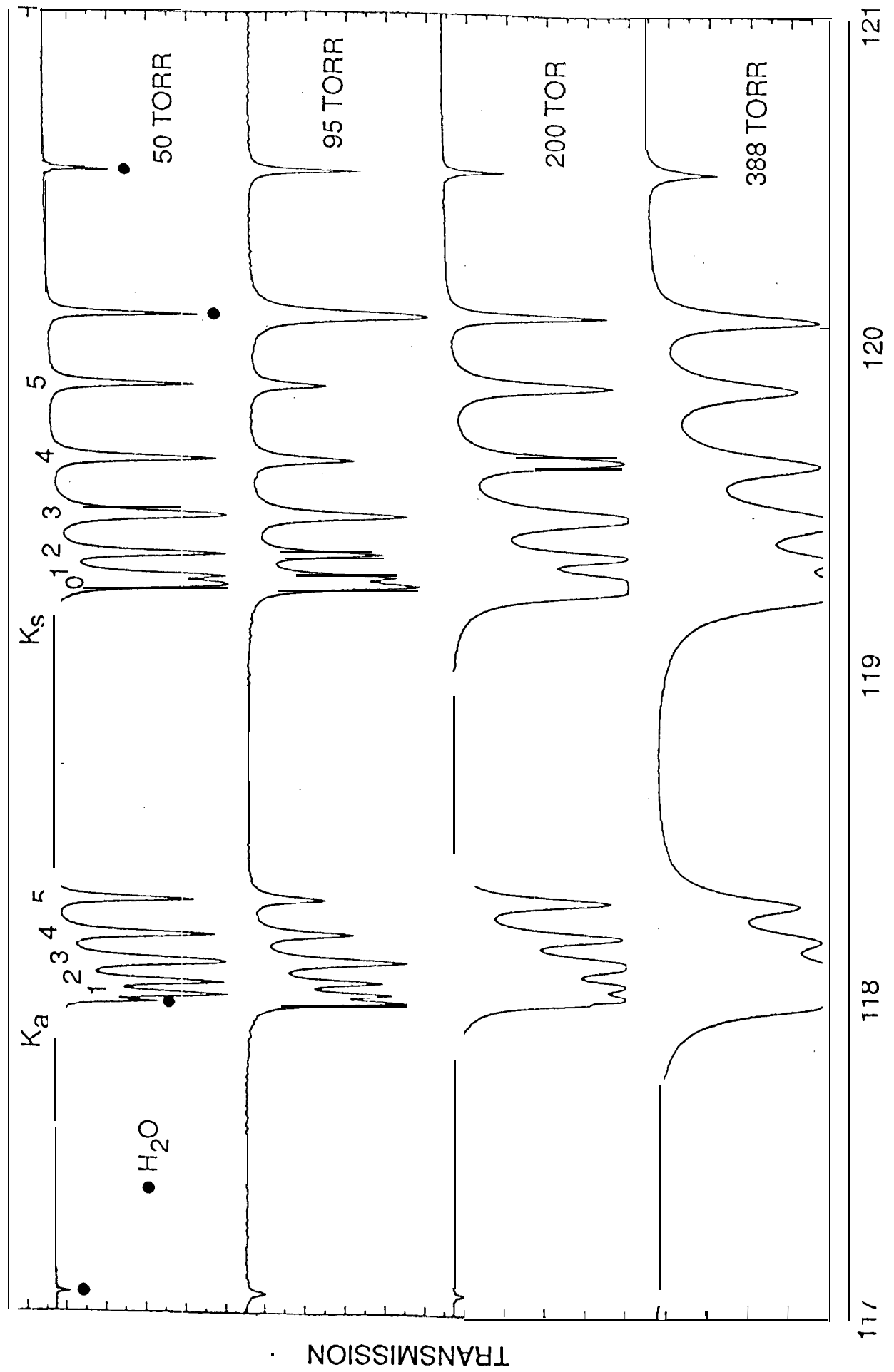
A, δ delta

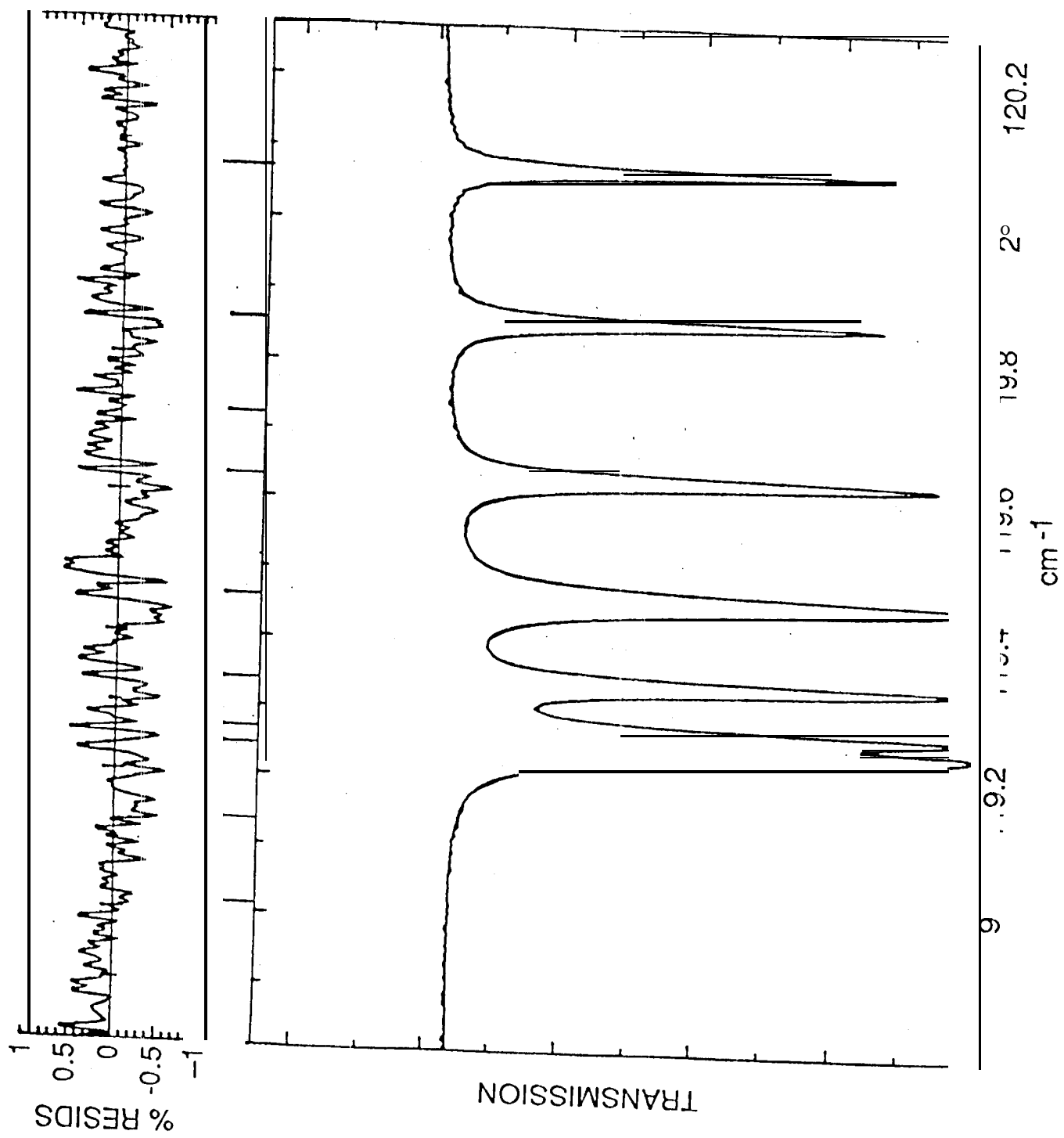
|| absolute value

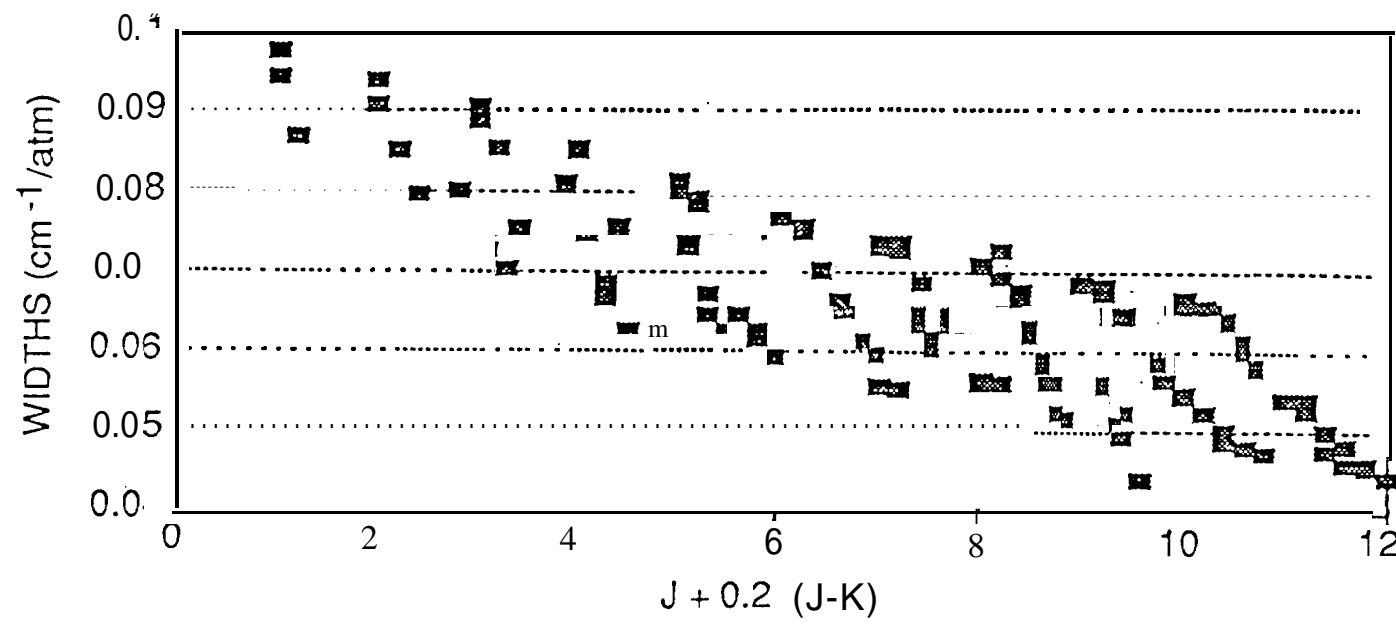
TRANSMISSION



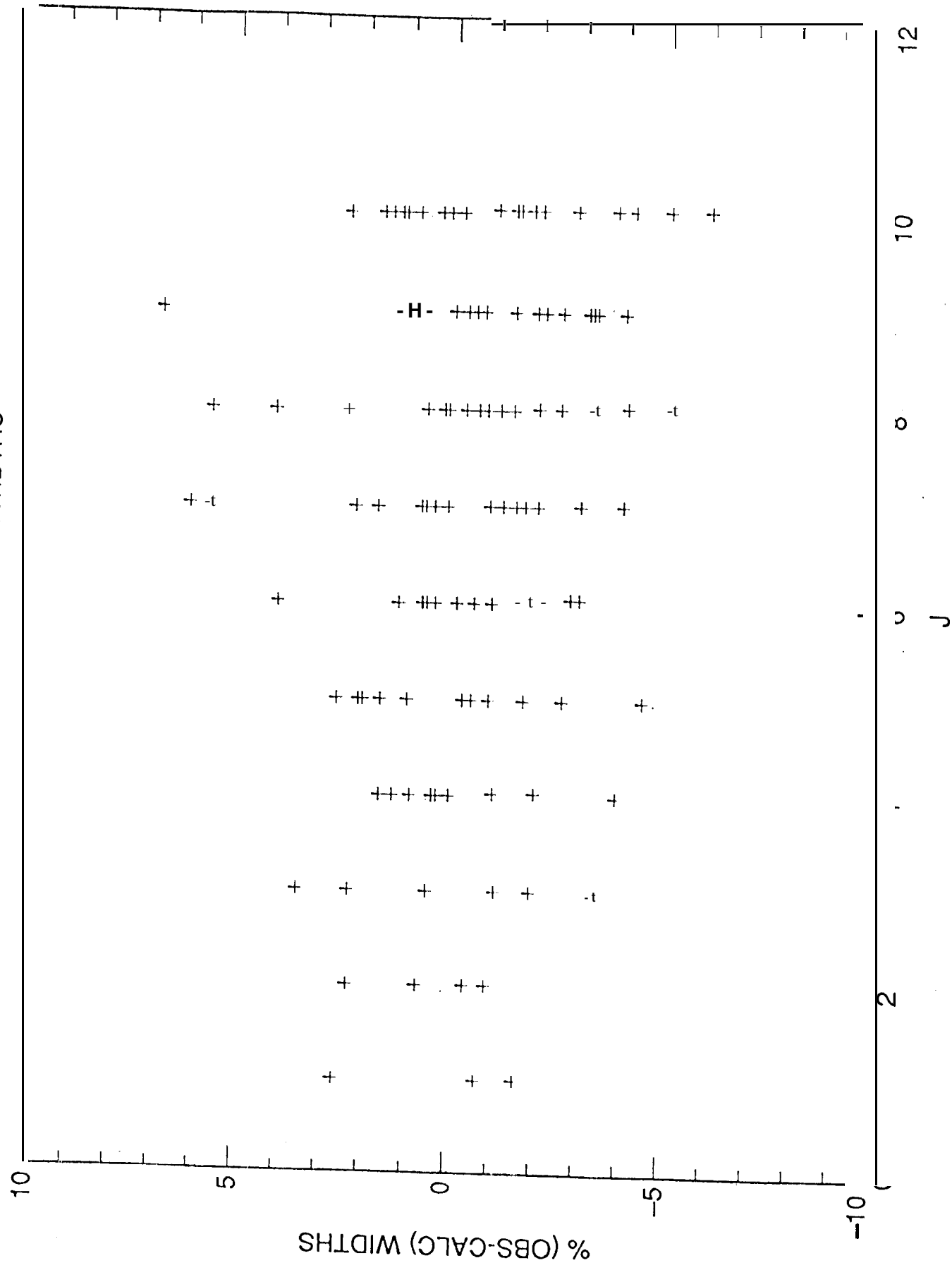
R₅ OF $^{14}\text{NH}_3$







PRESENT AMMONIA WIDTHS



TABLES

- I. Experimental Conditions of the Ammonia Spectra
- II. Retrieved Parameters for R_s from Two Pure NH_3 Spectra
- III. The Far-Infrared H_2 - and Self-broadened Widths of $^{14}\text{NII}_3$
- IV. Fitted R and Q Branch widths of v ,
- V. Fitted Constants for Equation 1 in units of $\text{cm}^{-1}/\text{atm}$
- VI. Rand Q Branch Widths of v_1 with the Same $|m|$
- VII. Vibrational or Temperature Dependence?

SYMBOLS

v nu

μ mu

Δ, δ delta

|| absolute value

Table] Experimental Conditions for the Ammonia Spectra

T o m	NH ₃	TORR I I ₂	PATH M	TEMP K
	3.995		0.0106	294.3
	20.00		0.0106	293.6
	0.320	49,9	0.263	297.0
	0.160	85.2	0.263	297.1
	1.01	94.5	0.263	298.0
	0,370	147,5	0.263	293.6
	1.04	203.0	0,263	298.0
	0.350	388.0	0,263	294.1"

Table 11 Retrieved Parameters for R_s from Two Pure JH₃ spectra

trans.	v cm ⁻¹	Δv 10^4	Intensity cm ⁻² /atm	%dif	Width cm ⁻¹ /atm	%dif
J" K"						
5 5	118.2417.	1	2.94	0.7	0.646	0.7
5 4	118.1760	1	4.49	0.0	0.574	0.0
5 3	118.0917	0	10.5	0.4	0.497	0.4
5 2	118.0309	1	5.74	1.0	0.412	4.6
5 1	117.9940	2	5.91	0.2	0.352	2.8
	L	-	-	-	-	-

Differences Between Measured Inversion Pairs

R S manifolds	K" = 5	K" = 4	K" = 3	K" = 2	K" = 1
A intensities	170	1%	K - - - b %		4%
A self-widths	1%	1 %	1%	2%	2%

TABLE 111 The Far-Infrared H₂- and Self - Broadened Widths of ¹⁴NH₃

Assignment sAJ	cm ⁻¹	Int	%err	Ic/lob	nun	H ₂ - width	%err	%0-c	self- width	%err	%0-c
aR 1 0	40.5229	1.980	5.1	1.042	4	0.0868	3.1	-1.6	0.240	8.0	-47.4
aR 1 1	38.9763	0.730	6.2	0.999	6	0.0975	3.5	2.6	0.361	8.0	-33.5
sR 1 1	40.5371	0.780	6.6	1.001	6	0.0943	6.0	-0.7	0.583	8.0	7.3
sR 2 0	58.8255	3.340	7.3	1.539	6	0.0796	4.8	0.7	0.331	8.0	-19.8
sR 2 1	60.3396	2.480	6.5	0.987	6	0.0850	3.2	-0.4	0.405	8.0	-18.3
sR 2 2	58.8333	2.210	5.3	0.691	2	0.0908	0.4	-0.9	0.777	8.0	34.3
OR ? 2	60.3874	1.660	3.4	0.972	6	0.0938	2.2	2.3	0.652	8.0	12.7
aR 3 0	80.0562	9.360	7.0	0.964	5	0.0702	2.9	-1.1	0.347	0.8	-6.6
aR 3 1	78.6277	3.940	9.5	1.057	6	0.0725	5.6	-5.5	0.393	3.4	-12.6
sR 3 1	80.0745	4.370	7.5	0.988	5	0.0753	3.4	-1.9	0.386	5.1	-14.2
s R3 2	78.6443	3.640	9.9	0.967	4	0.0798	6.0	-3.4	0.514	0.9	-2.7
aR 3 2	80.1305	3.680	5.5	0.996	5	0.0855	1.6	3.5	0.519	1.8	-1.8
a R 3 3	78.6728	4.620	3.1	0.972	6	0.0904	2.0	2.3	0.651	1.5	7.3
s R 3 3	80.2261	4.580	5.7	1.018	6	0.0888	1.6	0.5	0.631	1.4	4.0
s R 4 0	98.3472	11.700	0.6	0.946	2	0.0626	5.8	-2.0	0.373	6.6	12.5
aR 4 1	98.3584	5.450	2.6	0.993	3	0.0686	2.4	-0.9	0.403	6.0	-0.6
sR 4 1	99.7234	5.550	4.5	1.005	6	0.0665	2.5	-3.9	0.403	6.0	-0.6
s R4 2	98.3833	5.400	5.1	0.928	3	0.0755	2.8	1.3	0.540	10.0	12.6
aR 4 2	99.7868	5.180	4.5	0.995	6	0.0748	1.3	0.4	0.477	2.2	-0.5
aR 4 3	98.6281	8.410	4.2	0.993	4	0.0806	3.5	0.9	0.542	5.1	-2.1
s R 4 3	99.8951	8.490	4.4	1.013	6	0.0811	1.7	1.6	0.563	3.1	1.7
sR 4 4	98.4892	2.770	5.5	0.966	5	0.0854	1.9	0.3	0.668	1.6	6.5
aR 4 4	100.0492	2.820	7.2	0.973	6	0.0852	3.4	0.0	0.636	2.0	1.4
aR 5 0	119.2451	11.600	4.4	1.003	5	0.0591	3.4	2.1	0.321	12.1	9.5
aR 5 1	117.9935	5.990	7.0	0.935	6	0.0616	7.3	-1.7	0.368	7.2	1.5
sR 5 1	119.2696	5.750	9.4	0.996	5	0.0624	3.6	-0.5	0.358	13.9	-1.3
sR 5 2	118.0302	5.500	4.8	0.984	5	0.0645	3.7	-4.5	0.424	7.4	-1.9
aR 5 2	119.3394	5.700	4.6	0.971	6	0.0673	1.2	-0.3	0.443	4.1	2.5
a R 5 3	118.0913	9.890	4.5	1.010	6	0.0738	1.7	2.0	0.510	2.9	1.7
s R 5 3	119.4598	10.200	3.9	1.002	6	0.0731	3.2	1.0	0.517	1.5	3.0
s R 5 4	118.1753	4.240	4.8	0.992	6	0.0792	1.9	2.6	0.583	1.5	2.1
aR 5 4	119.6311	4.340	5.2	0.993	6	0.0784	1.7	1.6	0.577	1.5	1.0
a R 5 5	118.2814	2.760	4.3	0.986	6	0.0813	1.4	-0.9	0.655	0.6	2.2
s R 5 5	119.8573	2.800	4.8	1.001	6	0.0799	1.2	-2.6	0.642	2.1	0.2
SR 6 0-	137.5042	9.680	8.5	0.999	6	0.0550	4.4	4.0	0.339	9.5	32.4
aR 6 1	137.5202	4.990	8.0	0.963	4	0.0595	1.8	4.0	0.362	4.0	12.7
S R 6 1	138.6956	4.970	4.1	0.988	6	0.0555	2.6	-3.0	0.351	7.1	9.3
s R 6 2	137.5657	5.100	5.7	0.934	6	0.0613	1.4	-0.4	0.396	5.3	2.5
a R 6 2	138.7725	4.990	4.0	0.975	6	0.0611	1.2	-0.8	0.402	5.4	4.1
a R 6 3	137.6433	9.280	3.9	0.999	6	0.0651	2.7	-1.2	0.466	4.9	3.2
s R6 3	138.9035	9.400	4.0	1.008	6	0.0661	2.2	0.3	0.465	3.6	3.0
s R6 4	137.7498	4.370	4.1	0.993	6	0.0703	1.6	0.1	0.522	3.7	1.1
a R 6 4	139.0908	4.440	3.7	0.998	6	0.0700	1.2	-0.4	0.518	3.9	0.3
a R 6 5	137.8854	3.730	4.5	0.995	6	0.0755	1.4	1.2	0.584	3.1	0.4
s R6 5	139.3370	3.790	4.1	1.005	6	0.0749	1.8	0.4	0.581	2.6	-0.1
S R 6 6	138.0481	4.900	4.3	1.006	6	0.0774	1.1	-1.9	0.648	1.9	0.2
a R 6 6	139.6476	5.010	4.2	1.009	6	0.0767	1.2	-2.8	0.644	2.3	-0.4
a R 7 0	157.9591	6.970	8.8	1.024	5	0.0517	8.0	5.6	0.288	1.7	30.5
a R 7 1	156.9172	3.650	4.1	0.972	5	0.0521	3.2	-1.3	0.286	5.5	1.7
s R 7 1	157.9864	3.670	3.8	0.974	5	0.0560	6.1	6.1	0.285	1.6	1.3
s R7 2	156.9722	3.640	4.0	0.974	5	0.0560	2.3	-1.1	0.338	4.2	-1.2
aR 7 2	158.0708	3.670	4.5	0.979	5	0.0562	2.7	-0.8	0.341	3.4	-0.3
a R 7 3	157.0640	7.130	4.9	1.001	5	0.0615	7.6	1.7	0.389	0.6	-3.4
s R 7 3	158.2134	7.230	4.5	1.000	5	0.0602	5.0	-0.5	0.398	1.9	-1.1
s R 7 4	157.1934	3.580	4.0	0.988	5	0.0644	2.0	0.1	0.454	1.6	-2.0
a R 7 4	158.4138	3.630	4.1	0.981	5	0.0633	2.4	-1.6	0.449	2.2	-3.1
a R 7 5	157.3575	3.400	4.4	0.991	5	0.0687	1.9	0.7	0.511	1.3	-2.5
s R 7 5	158.6786	3.470	4.1	0.984	5	0.0685	2.3	0.4	0.510	1.6	-2.7
s R7 6	157.5563	6.000	4.5	0.986	5	0.0736	4.7	2.2	0.574	1.3	-1.8
aR 7 6	159.0114	6.020	3.8	1.005	5	0.0725	1.7	0.6	0.569	1.0	-2.7
a R 7 7	157.7865	1.990	5.3	1.007	5	0.0729	2.6	-4.0	0.638	0.6	-1.1
s R 7 7	159.4189	2.050	4.8	1.000	5	0.0738	2.6	-2.8	0.629	1.5	-2.5

TABLE III (continued)

Assignment		cm"	Int	%err	Ic/Iob	nun	H_2 -width	%err	%0-c	self-width	%err	%0-c
sAJ J" K"												
S R 8 0	176.1463	5.620	6.7	0.799	4	0.0437	7.2	-5.1	0.297	21.8	59.1	
aR 8 1	176.1680	2.330	5.7	0.963	5	0.0522	5.5	5.6	0.234	3.3	-3.7	
S R 8 1	177.1299	2.320	3.1	0.978	5	0.0491	4.1	-0.6	0.238	2.4	-2.0	
s R 8 2	176.2318	2.370	3.8	0.964	5	0.0529	3.5	0.2	0.285	0.7	-4.7	
aR 8 2	177.2199	2.320	4.2	0.994	5	0.0507	4.5	-3.9	0.289	0.2	-3.4	
a R 8 3	176.3405	4.730	3.6	0.984	5	0.0558	2.4	-0.6	0.336	2.5	-5.4	
s R 8 3	177.3692	4.870	3.1	0.972	4	0.0555	4.1	-1.1	0.334	1.3	-6.0	
sR 8 4	176.4887	2.420	3.3	0.986	5	0.0590	2.4	-0.8	0.395	0.1	-4.0	
aR 8 4	177.5859	2.460	3.9	0.983	5	0.0582	3.6	-2.2	0.399	0.9	-3.0	
a R 8 5	176.6803	2.450	3.5	0.986	5	0.0629	2.3	0.1	0.447	0.7	-4.4	
s R 8 5	177.8677	2.450	3.5	0.999	5	0.0620	1.3	-1.4	0.444	1.4	-5.1	
S R 8 6	176.9134	4.780	3.1	0.991	4	0.0678	1.4	2.4	0.520	0.8	-0.7	
aR 8 6	178.2211	4.810	2.6	0.998	6	0.0666	2.9	0.6	0.498	0.5	-4.9	
aR 8 7	177.1863	2.210	4.8	0.963	5	0.0724	4.0	4.1	0.552	1.0	-4.8	
s R 8 7	178.6528	2.130	5.3	1.015	6	0.0694	3.2	-0.3	0.556	0.6	-4.2	
S R 8 8	177.4969	1.500	5.5	1.000	5	0.0705	3.9	-3.3	0.618	2.6	-2.9	
a R 8 8	179.1703	1.510	3.6	1.006	6	0.0710	2.2	-2.7	0.619	0.7	-2.7	
a R 9 0	196.0793	2.700	5.6	0.928	6	0.0472	6.2	6.8	0.164	0.5	6.3	
aR 9 1	195.2559	1.310	4.7	0.958	5	0.0476	7.8	1.1	0.196	2.7	-4.9	
s R 9 2	195.3282	1.320	3.1	0.965	5	0.0484	5.3	-3.1	0.243	3.6	-5.7	
aR 9 2	196.2059	1.370	5.9	0.943	6	0.0497	5.9	-0.5	0.243	1.5	-5.7	
aR 9 3	195.4467	2.730	3.2	0.972	5	0.0519	5.0	-1.7	0.286	0.7	-7.6	
s R 9 3	196.3696	2.780	2.7	0.961	6	0.0522	3.9	-1.2	0.287	0.3	-7.3	
sR 9 4	195.6190	1.410	3.7	0.979	5	0.0544	3.6	-2.3	0.342	2.0	-5.3	
aR 9 4	196.5936	1.420	4.3	0.983	6	0.0540	4.6	-3.0	0.345	1.3	-4.5	
aR 9 5	195.8367	1.430	2.2	1.011	4	0.0562	2.0	-4.0	0.393	1.4	-4.8	
s R 9 5	196.8915	1.500	4.3	0.982	6	0.0585	4.3	-0.1	0.401	1.7	-2.9	
a R 9 7	196.4160	1.510	6.0	1.005	6	0.0644	5.3	0.2	0.505	0.1	-2.2	
SR 9 7	197.7173	1.540	3.6	1.003	6	0.0641	3.1	-0.3	0.503	0.1	-2.6	
s R 9 8	196.7747	1.400	4.7	1.007	6	0.0680	4.8	1.2	0.558	0.6	-1.8	
a R 9 8	198.2589	1.410	2.5	1.020	6	0.0673	2.1	0.2	0.557	0.7	-2.0	
a R 9 9	197.1766	2.010	3.2	1.008	6	0.0687	2.8	-1.9	0.620	0.1	0.0	
s R 9 9	198.8998	2.030	3.4	1.018	6	0.0680	2.7	-2.9	0.618	0.2	-0.3	
SR 10 0	214.1397	1.260	3.9	0.971	5	0.0442	5.0	1.9	0.159	7.7	29.0	
SR 10 1	214.9169	0.640	2.3	0.977	6	0.0458	6.0	0.1	0.175	4.8	2.6	
aR 10 1	214.1665	0.650	7.4	0.953	5	0.0454	8.0	-0.8	0.151	11.5	-11.5	
sR 10 2	214.2469	0.670	5.1	0.948	5	0.0482	10.3	0.1	0.208	0.1	-4.5	
aR 10 2	215.0173	0.640	5.6	0.995	6	0.0460	7.6	-4.5	0.209	1.7	-4.1	
SR 10 3	215.1805	1.400	3.0	0.955	6	0.0498	6.3	-1.4	0.258	2.0	-2.7	
aR 10 3	214.3856	1.330	3.4	0.911	5	0.0475	7.3	-6.0	0.244	3.2	-8.0	
SR 10 4	214.5692	0.740	9.5	0.940	5	0.0523	6.2	-1.2	0.286	5.4	-8.5	
aR 10 4	215.4254	0.750	7.8	0.934	6	0.0537	5.1	1.5	0.308	2.8	-1.4	
sR 10 5	215.7373	0.770	1.4	0.988	6	0.0538	2.5	-2.7	0.353	1.9	-1.9	
aR 10 5	214.8123	0.740	3.5	1.006	6	0.0536	4.9	-3.1	0.359	2.1	-0.2	
sR 10 6	215.1088	1.650	5.2	0.984	6	0.0579	5.9	0.4	0.410	3.6	0.7	
aR 10 6	216.1271	1.650	4.0	0.996	6	0.0580	4.8	0.6	0.403	1.7	-1.0	
SR 10 7	216.6002	0.880	3.5	1.000	6	0.0598	3.3	-0.4	0.453	0.7	-0.3	
aR 10 7	215.4594	0.850	8.1	1.022	6	0.0611	5.0	1.7	0.458	1.9	0.8	
SR 10 8	215.8634	0.890	2.7	1.008	6	0.0639	3.2	2.4	0.518	3.4	3.2	
aR 10 8	217.1645	0.920	3.9	0.990	6	0.0636	4.5	1.9	0.516	1.3	2.9	
SR 10 9	217.8287	1.730	3.4,	1.006	6	0.0657	3.0	1.4	0.557	0.5	1.5	
aR 10 9	216.3192	1.630	3.6	1.052	6	0.0655	4.4	1.1	0.531	0.7	-3.3	
SR 10 10	216.8242	0.620	3.8	1.029	6	0.0657	5.4	-2.2	0.622	1.9	4.3	
aR 10 10	218.6073	0.640	6.3	1.006	6	0.0666	4.7	-0.9	0.622	1.1	4.3	

* Intensities are in units of cm^2/atm , and widths are in $\text{cm}^{-1}/\text{atm}$ at 296 K. Ic/Iob is the ratio of the calculated and observed intensities.

TABLE 1 V Fitted R and Q Branch widths of v,

Assignments	AJ	J"	K"	positions	N₂ cm ⁻¹	widths	%o-c	O₂ widths	%o-c	Ar widths	%o-c	H₂ widths	%o-c	He widths	%o-c	NH₃ widths	%o-c
a R 0 0				3355.00569	1.131	-4.4	0.646	-5.4	0.494	-6.0	0.984	-2.6	0.344	-5.5	3.306	-23.7	
s R 1 0				3376.26860	1.067	-2.6	0.617	-3.9	0.489	-3.3	0.872	-3.4	0.311	-7.3	2.492	-28.8	
a R 1 1				3374.55009	1.154	0.5	0.673	1.7	0.538	2.9	0.981	0.8	0.363	3.0	5.163	0.6	
sR 1 1				3376.32483	1.154	0.5	0.673	1.7	0.539	3.1	0.974	0.1	0.362	2.8	5.247	2.3	
aQ 1 1				3335.17119	1.116	-2.8	0.635	-4.1	0.489	-6.5	0.906	-6.9	0.342	-2.9	5.796	13.0	
sQ 1 1				3336.95178	1.145	-0.3	0.659	-0.5	0.509	-2.7	0.965	-0.8	0.362	2.8	5.849	14.0	
sQ 2 1				3336.56026	1.101	3.1	0.657	5.2	0.526	4.8	0.921	5.1	0.330	1.2	3.910	-9.0	
a Q 2 2				3334.93295	1.137	2.0	0.659	2.8	0.534	3.1	0.929	-0.8	0.341	0.2	6.411	11.2	
s Q 2 2				3336.71601	1.124	0.8	0.652	1.7	0.535	3.2	0.920	-1.7	0.339	-0.4	6.267	8.7	
s R 3 0				3414.63602	0.973	1.4	0.551	-4.8	0.461	-0.9	0.718	-4.4	0.281	-4.1	3.013	30.3	
aR 3 1				3412.95890	1.009	0.9	0.575	-3.0	0.468	-2.6	0.762	-4.9	0.290	-4.8	3.741	3.4	
s R 3 1				3414.68325	1.013	1.3	0.578	-2.5	0.472	-1.8	0.771	-3.7	0.290	-4.8	3.814	5.4	
a R 3 2				3413.08717	1.086	4.4	0.627	3.4	0.507	2.3	0.874	2.7	0.336	6.2	4.969	0	
aQ 3 1				3334.27940	0.922	-7.8	0.575	-3.0	0.480	-0.1	0.734	-8.4	0.289	-5.2	3.165	-12.5	
5 9 3 1				3336.00065	0.949	-5.1	0.573	-3.3	0.485	0.9	0.723	-9.7	0.303	-0.6	3.327	-8.1	
s R3 2				3414.83238	1.071	2.9	0.616	1.6	0.497	0.2	0.857	0.7	0.320	1.1	4.979	1.1	
aQ 3 2				3334.39309	1.051	1.0	0.638	5.2	0.524	5.7	0.887	4.2	0.349	10.3	4.845	-1.7	
sQ 3 2				3336.13887	1.081	3.9	0.657	8.4	0.535	7.9	0.910	6.9	0.357	12.8	5.026	2.0	
a R 3 3				3413.32029	1.126	4.1	0.636	2.6	0.515	0.7	0.911	1.1	0.331	0.8	6.193	-0.7	
s R 3 3				3415.10498	1.116	3.2	0.626	1.0	0.512	0.2	0.903	0.2	0.330	0.5	6.227	-0.1	
a Q 3 3				3334.59821	1.074	-0.7	0.607	-2.1	0.502	-1.8	0.865	-4.0	0.319	-2.8	6.364	2.1	
sQ 3 3				3336.39038	1.093	1.1	0.623	0.5	0.515	0.7	0.876	-2.8	0.330	0.5	6.476	3.9	
aQ 4 2				3333.71824	0.988	0.9	0.631	9.3	0.511	8.0	0.827	5.1	0.318	6.9	4.340	2.2	
sQ 4 2				3335.42557	0.995	1.6	0.601	4.1	0.469	-0.9	0.808	2.7	0.306	2.9	4.332	2.0	
a Q 4 3				3333.89032	1.013	-0.1	0.593	0.8	0.481	-1.3	0.863	4.4	0.324	5.6	5.327	-1.2	
s Q 4 3				3335.63575	1.024	1.0	0.592	0.7	0.480	-1.5	0.860	4.0	0.313	2.1	5.365	-0.5	
aQ 4 4				3334.16797	1.046	-0.2	0.594	-0.8	0.504	0.4	0.832	-4.0	0.303	-4.1	6.446	-1.4	
s Q 4 4				3335.97588	1.059	1.0	0.596	-0.4	0.509	1.4	0.832	-4.0	0.301	-4.7	6.422	-1.8	
s o5 2				3334.64270	0.990	6.5	0.590	6.3	0.465	3.4	0.746	0.4	0.290	2.4	3.992	7.2	
a o5 3				3333.08621	0.948	-1.1	0.562	-0.1	0.459	-1.0	0.767	-0.8	0.290	0.0	4.698	-0.2	
sQ 5 3				3334.79249	0.987	3.0	0.561	-0.2	0.451	-2.7	0.769	-0.6	0.291	0.4	4.768	1.3	
aQ 5 4				3333.30315	0.986	-0.1	0.585	2.7	0.489	2.5	0.828	3.0	0.321	8.2	5.888	3.5	
s Q 5 4				3335.05558	1.002	1.5	0.573	0.6	0.462	-3.2	0.819	1.9	0.294	-0.9	5.582	-1.9	
a Q 5 5				3333.64439	0.996	-1.9	0.569	-1.4	0.497	1.3	0.792	-5.0	0.291	-4.1	6.387	-4.3	
s Q 5 5				3335.47564	1.002	-1.3	0.568	-1.6	0.489	-0.3	0.789	-5.4	0.285	-6.1	6.405	-4.0	
aQ 6 3				3332.27009	0.934	2.1	0.539	-0.7	0.454	3.4	0.746	0.6	0.286	2.9	4.429	5.9	
s Q 6 3				3333.97347	0.862	-5.8	0.521	-4.0	0.425	-2.3	0.705	-4.9	0.270	-2.8	4.172	-0.2	
a Q 6 4				3332.39832	0.926	-1.2	0.527	-3.7	0.416	-7.9	0.756	-0.7	0.274	-2.9	4.973	-0.6	
s Q 6 4				3334.12327	0.930	-0.8	0.536	-2.0	0.421	-6.8	0.743	-2.4	0.272	-3.6	4.891	-2.2	
a Q 6 5				3332.64002	0.957	-0.3	0.536	-2.8	0.453	-2.5	0.764	-2.3	0.278	-3.0	5.604	-3.8	
s o6 5				3334.41434	0.968	0.8	0.548	-0.6	0.447	-3.7	0.804	2.9	0.279	-2.6	5.566	-4.5	
a Q 6 6				3333.02495	0.946	-3.7	0.535	-3.7	0.472	-1.1	0.753	-6.1	0.285	-2.0	6.321	-4.9	
S Q 6 6				3334.90113	0.962	-2.1	0.529	-4.8	0.468	-1.9	0.748	-6.7	0.279	-4.1	6.459	-2.8	
a Q 7 5				3331.71342	0.880	-4.1	0.497	-6.5	0.390	-10.9	0.717	-4.5	0.252	-8.1	4.945	-3.7	
s Q 7 5				3333.49896	0.878	-4.3	0.515	-3.1	0.451	3.0	0.709	-5.5	0.263	-4.1	4.935	-3.9	
aQ 7 6				3331.92377	0.942	0.9	0.542	1.8	0.468	4.1	0.776	2.0	0.295	6.8	5.964	2.9	
s o7 6				3333.57292	0.932	-0.2	0.530	-0.5	0.435	-3.2	0.782	2.8	0.266	-3.7	5.630	-2.8	
a Q 7 7				3332.34862	0.915	-3.7	0.511	-4.3	0.453	-1.8	0.735	-4.7	0.266	-4.3	6.413	-0.6	
s Q 7 7				3334.25888	0.946	-0.5	0.526	-1.5	0.465	0.8	0.756	-2.0	0.267	-3.9	6.391	-1.0	
s o8 5				3333.42110	0.859	-3.1	0.555	7.2	0.447	8.9	0.738	-0.4	0.265	-0.7	4.263	-7.4	
a Q 8 6				3331.03779	0.884	-1.5	0.498	-3.4	0.400	-5.1	0.720	-2.8	0.249	-6.5	5.166	1.3	
sQ 8 6				3332.93806	0.882	-1.7	0.487	-5.6	0.386	-8.4	0.731	-1.3	0.243	-8.7	4.955	-2.8	
aQ 8 7				3331.17793	0.879	-3.2	0.498	-3.1	0.419	-3.1	0.741	-0.1	0.254	-4.3	5.331	-4.8	
aQ 8 8				3331.62842	0.939	2.3	0.527	3.0	0.476	7.3	0.761	2.6	0.287	8.4	6.566	7.7	
S Q 8 8				3333.50989	0.878	-4.4	0.515	0.6	0.451	1.7	0.709	-4.4	0.263	-0.7	6.158	1.0	
a Q 9 6				3:531.73845	0.943	8.0	0.526	4.2	0.442	12.4	0.747	0.7	0.292	11.8	4.781	4.8	
a Q 9 8				3332.25386	0.912	3.4	0.503	1.7	0.378	-8.6	0.696	-3.7	0.232	-8.9	5.475	4.6	
a Q 9 9				3332.63173	0.957	8.0	0.536	9.4	0.453	7.0	0.764	7.1	0.278	10.5	5.815	4.4	

+ the observed widths from Pine et al. [81] and Markov et al. [9] are in units of cm⁻¹/MPa at 296 K (1 cm⁻¹/atm = 0.101325 cm⁻¹/MPa).

Table V Fitted Constants for Equation 1 in units of $\text{cm}^{-1}/\text{atm}$

Study	a_0	a_1	a_2	a_3	a_4	% obs -cal	# mess.
H ₂ - present	0.09839 (15)	-0.01071 (31)	0.00728 (29)	0.000521 (29)	-0.039490 (34)	2.4	116
Pine et al.	0.1011 (33)	-0.0118 (12)	0.0079 (12)	0.00106 (19)	-0.00099 (20)	3.9	58
Self- present	0.500 (26)	-0.0452 (78)	0.0918 (63)	0.00075 (66)	-0.09445 (72)	11.2	116
Markov et al.	0.433 (34)	-0.091 (28)	0.179 (13)	0.0079 (20)	-0.0169 (22)	8.0	58
N ₂ - Pine et al.	0.1182 (32)	-0.0093 (12)	0.0059 (12)	0.00062 (1s)	-0.00061 (20)	3.2	58
O ₂ - Pine et al.	0.0682 (34)	-0.00437 (83)	0.00230 (s4)	0.000303 (13)	-0.00031 (14)	3.8	58
He- Pine et al.	0.0364 (16)	-0.00309 (59)	0.00193 (59)	0.000240 (91)	-0.00025 (lo)	5.2	58
Ar- pine et al.	0.0526 (21)	-0.00195 (80)	0.001s0 (s1)	-0.000021 (12)	-0.00088 (13)	4.8	5s
H ₂ - Margolis R and Q Poynter P	0.13s5 (34) 0.1423 (42) 0.1615 (33)	-0.01%?3 (s9) -0.0195 (16) -0.02391 (97)	0.01234 (79) 0.0124 (12) 0.01714 (94)	0.00091s (ss) 0.00101 (15) 0.00134 (73)	-0.00074 (88) -0.00777 (90) -0.00134 (110)	4.5 4.2 4.7	85 50 6s

TABLE VI R and Q branch widths of v, with the Same |m|

	J''	m	K''	N ₂	O ₂	Ar	H ₂	He	NH ₃
aR	1	2	1	1.154	0.673	0.538	0.981	0.363	5.163
sR	1	2	1	1.154	0.673	0.539	0.974	0.362	5.247
sQ	2	2	1	1.101	0.657	0.526	0.921	0.330	3.910
%dif (R-Q)				4.5	2.4	2.3	6.5	9.7	33.
aR	3	4	2	1.086	0.627	0.507	0.874	0.336	4.969
aQ	4	4	2	0.988	0.631	0.511	0.827	0.318	4.340
sQ	4	4	2	0.995	0.601	0.469	0.808	0.306	4.332
%dif (R-Q)				9.5	1.8	3.7	6.8	7.7	15.
aR	3	4	3	1.126	0.636	0.515	0.911	0.331	6.193
sR	3	4	3	1.116	0.626	0.512	0.903	0.330	6.227
aQ	4	4	3	1.013	0.593	0.481	0.863	0.324	5.327
sQ	4	4	3	1.024	0.592	0.480	0.860	0.313	5.365
%dif (R-Q)				10.0	6.5	6.6	5.2	3.8	16.3

* The widths are in cm⁻¹/MPa at 296 K from Pine et al. [8] and Markov et al. [9]. m = J+1 for R, m = -J for Q and m = -J for P. The quantity %dif is the difference between widths of the same value of |m|.

Table VII Vibrational or Temperature Dependence?⁺

Assignment	Rotational H ₂ -width	v ₂ H ₂ -width	ratio v ₂ /rot.	n (± 0.1)
R (4,4)	0.0854	0.1182	1.38	0.82
R (4,3)	0.0809	0.1123	1.39	0.85
R (4,2)	0.0752	0.0970	1.29	0.65
R (4,1)	0.0675	0.0852	1.26	0.60
R (4,0)	0.0626	0.0800	1.28	0.63
R (6,6)	0.0770	0.113	1.4s	0.96
R (6,5)	0.0753	0.102	1.36	0.78
R (6,4)	0.0701	0.0915	1.31	0.68
R (6,3)	0.0656	0.0838	1.26	0.60
R (6,2)	0.0612	0.0751	1.23	0.52
R (6,1)	0.0575	0 . 0 6 9 2	1.12	0.30
R (6,0)	0.0550	0.0674	1.22	0.52

⁺The rotational widths in cm⁻¹/atm are at 296 (3) K and the v₂ widths from Margolis and Poynter [7] are at 200 K. The error estimate for n includes experimental uncertainties of widths and temperatures.